International Journal of Scientific & Engineering Research, Volume 4, Issue 8, August 2013
ISSN 2229-5518

Carbon di- Oxide Reduction In A SI Engine- Experimental And CFD Studies

Sajin George, D.Ganesh

Abstract— Besides the further reduction of the harmful gaseous emissions (HC, CO and NO_X) to meet stringent emission limits, the discussion on lowering the CO_2 emissions is omnipresent. Various solid materials like calcium oxide, zeolite, hydrotalcite, silicon carbide nanotubes are readily adsorb carbon dioxide. A new family of three way catalytic converter-technologies offers to tune the catalyst system to the engine performance and the back pressure requirement, which helps to minimizing CO_2 emissions. In addition, these technologies show improved performance in HC, CO, NO_X, light-off, and in CO and NO_X conversions under dynamic conditions-this again can positively impact the CO_2 emissions as less harsh heating strategies for start is required. A low exhaust back pressure and a fast light-off contribute to fuel reduction and with that to CO_2 reduction. Computer simulation is being increasingly used in the catalytic converter industry. The objective of the present work is to reduce CO_2 emissions by following methods (1) Enhancing the catalyst system to the engine performance and the back pressure (CFD Analysis) (2) Attaching chemical reagent system to the catalytic converter and thereby reducing CO_2 emissions from the exhaust. The reduction in exhaust gas back pressure of the exhaust system offers a possibility to reduce the CO_2 emissions as well as having improved power and torque characteristics of the engine. Hydrotalcite, zeolite , and silicon carbide nanotube, posses high rate of adsorption capacity of CO_2 at elevated temperatures. A converter of required size or configuration based on CFD results will be fabricated and tested with the above adsorbents.

Index Terms— Three Way Catalytic Converter(TWC), Spark Ignition(SI), Silicon Carbide Nanotube(SCNT), Double Overhead Camshaft(DOHC),Computational Fluid Dynamics(CFD)

1 INTRODUCTION

THE transport sector is one of the major contributors to greenhouse gas emissions. Reducing Carbon Dioxide (CO_2) [13] emissions is one of the major challenges for automobile manufacturers. The amount of carbon dioxide has increased by more than 30% since pre-industrial times and is still increasing at an unprecedented rate of on average 0.4% per year, mainly because of the combustion of fossil fuel [3].The increased CO_2 level is believed to enhance the greenhouse effect and its global adverse consequences. Significant climate changes are very likely associated with increased atmospheric concentrations of certain gases, most significantly CO_2. Globally there is an increasing concern over the environmental impact of anthropogenic gas emissions, particularly carbon dioxide, with targets and taxes being implemented to decrease gas release to the atmosphere. Tremendous reduction of hydrocarbons, carbon monoxide and nitric oxides emitted from internal combustion engines is today achieved by the application of automotive catalytic converters. The growing concern about the environmental impact of these pollutants have led to more and more restrictive regulations, which in turn have provided the impetus for the development of increasingly efficient exhaust gas after treatment systems and catalytic converters. Even in catalytic converter also CO is converted to CO_2, so there should be some technology to reduce CO_2. Also fuel efficiency improvements and CO_2 emission reduction can compensate for product cost, especially considering CO_2 emission tax and taking an overall holistic viewpoint.

1.1 CO_2 Reduction Using Adsorbents

Various solid materials readily adsorb carbon dioxide.[16] These materials can be classified as (i) microporous and mesoporous inorganic and organic materials such as zeolites, silica gel, alumina, and activated carbon, (ii) mixed oxide materials such as CaO (iii) lithium metal oxides such as lithium zirconate (LZC) and lithium orthosilicate (LOS) (iv) and hydrotalcite-like materials (HTC) . The first type of materials tends to show high physical adsorption rate for CO_2 with a reasonable high adsorption capacity at low temperature (near ambient). CO_2 working capacity drastically diminishes to be almost negligible as the temperature increases above 250°C. [7]. CaO has also been reported to show strong affinity for CO_2 sorption at high temperature above 500°C. CaO can react with CO_2 in a bulk chemical carbonation reaction according to:

$$CaO + CO_2 \Longleftrightarrow CaO_3 \quad \Delta H_{298K} = -182 \text{ kJ/mol}$$

CaO offers very high temperature-independent stoichiometric sorption capacity of 17.8 CO_2 mol/kg .However, CaO has also some operational limitations [7]:(i) the CO_2 working capacity is much lower than the stoichiometric capacity unless the material is regenerated at high temperature of 900°C due to the thermodynamically unfavorable desorption of CO_2, thus (ii) slow kinetics of sorption/desorption at low temperature of about 500°C, (iii) cyclic stability of CaO[12] in terms of CO_2 is significantly reduced due to the buildup of the irreversible $CaCO_3$. Lithium zirconate (LZC) and lithium orthosilicate (LOS) have recently received more attention due to their ability to retain good CO_2 chemisorption capacity at high temperature (5.0 mol/kg [10] and 6.13 mol/kg [10], respectively). However, the slow sorption kinetics and the high heat of reaction due to the strong chemical bonding to CO_2 require a high regeneration temperature (900°C for LZC [8] and 700°C for LOS[10], respectively

$$Li_2ZrO_3 + CO_2 \Longleftrightarrow Li_2CO_3 + ZrO_2 \quad \Delta H_{298K} = -160 \text{ kJ/mole}$$

$$Li_4SiO_4 + CO_2 \Longleftrightarrow Li_2SiO_3 + Li_2CO_3 \quad \Delta H_{298K} = -142 \text{ kJ/mole}$$

1.2 Catalytic Converter

Catalytic converters[11] have been used for about thirty five years to reduce the toxicity of exhaust emissions from the internal combustion engine. The majority of automotive catalytic converters have a monolithic structure,[2] which is coated with an alumina washcoat that supports the noble metal such as platinum, palladium and rhodium. Depending on system design and powertrain operating condition, approximately 30-

• *Sajin George completed M.Tech from Anna Universit Guindy,. E-mail: sajingr@gmail.co*

40% of the total exhaust system pressure loss occurs in the catalytic converter [14].

1.3 Fuel Consumption And CO_2 Emission

There is linear dependence between the emission of carbon dioxide (CO_2) and fuel consumption. Average fuel consumption and CO_2 emission of automobiles using diesel oil is lower than these characteristics of cars using petrol (but more when compared with 1 litre of fuel). Also if larger the engine displacement and automobile mass of an automobile, higher its fuel consumption and CO_2 emission. The Eco-Driving technique which includes measures such as preventing sudden acceleration and shifting-up at lower engine speed is attractive because it has an immediate effect on reduction of CO_2 emissions from vehicles with minimal effort. But as a general rule, higher the carbon dioxide emission reading, more efficient engine is operating. Ideal combustion produces more CO_2 and water vapor. At stoichiometric air-fuel ratio (14.7:1) CO_2 emission is more because of the complete combustion of fuel and air, at the same time CO and HC is less.

2 METHODOLOGY

2.1 Enhancing the Catalyst System

The reduction of exhaust gas back pressure of the exhaust system offers a possibility to reduce the CO_2 emissions as well as having improved power and torque characteristics of the engine. A 3% increase in the exhaust back pressure leads to a CO_2 increase of 0.5% [15].. Hence CFD analysis is used to design efficient catalytic converters:[9] By modeling the exhaust gas run rate, drop in pressure and the uniformity of flow through the substrate can be determined. This can be done by following methods

- Boundary conditions are given
- A model of the catalytic converter with typical dimension is created by using GAMBIT pre-processor
- The flow through the catalytic converter is considered as a flow through porous medium
- FLUENT is used to model the flow of nitrogen gas through catalytic converter geometry, so that the flow field structure can be analyzed

3. EXPERIMENTAL SETUP

3.1 Test Engine Details

For the experiments a four cylinder, four stroke petrol engine Hyundai i10 automatic transmission car is used. The car is equipped with catalytic converter with closed loop control system. The technical specifications are given in (See Table 3.1)

Table 3.1Engine Specifications

Engine Type/Model	1.2 Kaapa, 4-cylinder Petrol
Displacement cc	1197
Power (PS@rpm)	80PS @5200rpm
Torque (Nm@rpm)	111Nm @4000rpm
Bore (mm)	71
Stroke (mm)	75.6
Compression Ratio	10.5:1
No of Cylinders (cylinder)	4
Cylinder Configuration	Inline
Valves per Cylinder (value)	4
Fuel Type	Petrol

3.2 EXPERIMENTAL LAYOUT

(See Figure 3.1) show the PRO-E model of the experimental set up. Flow is taking place right to left, which is from the catalytic converter to the CO_2 adsorber system.

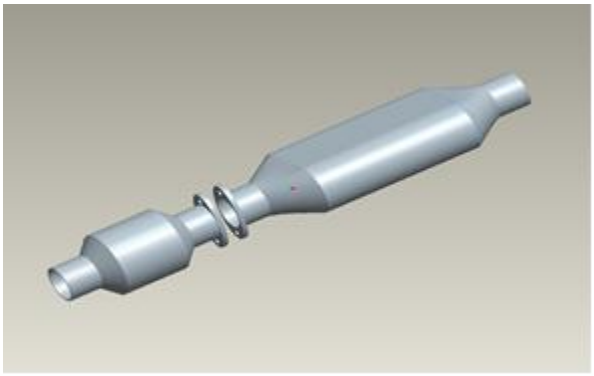

Figure 3.1 PRO-E Model of the Experimental Setup

CATALYTIC CONVERTER MODELLING

(See Figure 5.1) show the exhaust system of a typical 4-cylinder SI engine equipped with a TWC. The exhaust system consists of three distinct parts, which include (i)an exhaust manifold, (ii) an exhaust pipe and (iii) a catalytic converter.

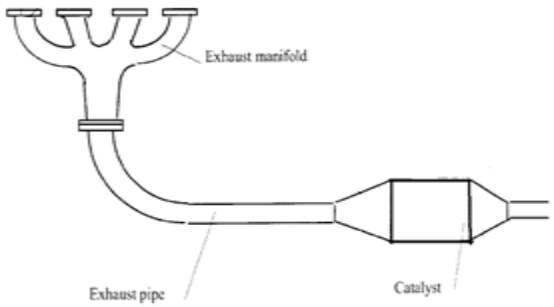

Figure 4 Exhaust System

The equations governing the fluid flow are the three fundamental principles of mass, momentum, and energy conservation

$$\frac{\partial_\rho}{\partial_t} + \nabla(\rho u) = 0 \qquad (1)$$

$$\rho\frac{DV}{DT} = \nabla\tau_{ij} - \nabla_p + \rho F \qquad (2)$$

$$\rho\frac{D_e}{D_t} + P(\nabla u) = \frac{\partial_Q}{\partial_t} - q + \emptyset \qquad (3)$$

Where ρ is the fluid density, *u* as the fluid velocity vector, τ_{ij} is used to represent viscous stress tensor, *p* is pressure, F represents the body forces, e can be the internal energy, *Q* the heat source , *t* is time, Φ as the dissipation term, and ∇.q is the heat loss by conduction. The flow in the upstream diffuser and manifolds is obtained through solution of the Reynolds-averaged Navier–Stokes (RANS) equations. The monolith itself is normally treated as a porous medium with properties (porosity, flow resistance, conductivity, thermal capacity, etc.) governed by the geometric configuration of the channels within the monolith and its material composition. [1]

4.1 Flow Through Porous Media

Modeling of flows through a porous medium requires a modified formulation of the Navier-Stokes equations, which reduces to their classical form and includes additional resistance terms induced by the porous region. The incompressible Navier-Stokes equations in a given domain Ω and interval (0,t) can be as follows:

$\rho(\partial u/\partial t + (u\cdot\nabla)u) - \mu\nabla^2 u + \nabla p = f$ on $\Omega x(0,t)$ (4)
$\nabla\cdot u = 0$ on $\Omega x(0,t)$

Where u = u(x,t) denotes the velocity vector, p = p(x,t) the pressure field, ρ the constant density, μ the dynamic viscosity coefficient and f represents the external body forces acting on the fluid (i.e. gravity). The general form of the Navier-Stokes equation is valid for the flow inside pores of the porous medium but its solution cannot be generalized to describe the flow in porous region. Therefore, the general form of Navier-Stokes equation must be modified to describe the flow through porous media. To this aim, Darcy's law is used to describe the linear relation between the velocity u and gradient of pressure p in the porous medium. It represents the permeability resistance of the flow in a porous media:

$\nabla p = -\mu D u$ in $\Omega_p x(0,t)$ (5)

Where Ω_p is the porous domain, D the Darcy's law resistance matrix and u the velocity vector. In the case of considering an homogeneous porous substrate, D is a diagonal matrix with coefficients 1/α, where α is the permeability coefficient. Considering a modified Navier-Stokes equation in the whole domain including the two source terms associated to the resistance induced by the porous medium (linear Darcy and inertial loss term), the momentum equations become

$\rho\,\partial u/\partial t - \mu\nabla^2 u + \nabla p - \mu D u - 0.5\,\rho C|u| = 0$ in $\Omega x(0,t)$

Therefore, the Navier-Stokes momentum equations can be rewritten as

$\rho\partial u/\partial t - \mu\nabla^2 u + \nabla p = -\mu D u$ in $\Omega x(0,t)$ (6)

5. RESULTS

5.1 Catalytic Converter CFD Modelling

Computational fluid dynamics is applied to calculate the pressure distribution, velocity field the uniformity of flow through the substrate in the inlet and outlet cone. GAMBIT 2.4 and FLUENT 6.3.26 is used for the analysis. Steps involved in this process are:

- Problem Identification(Define goals, Identify domain)
- Pre-processing(Geometry, Mesh, Physics)
- Solve(Compute solution)
- Post-processing(Examine results)

The existence of the monolith is simulated by a porous medium with a prescribed pressure drop. The flow through the monolith is treated as laminar and the pressure drop per unit length is calculated by using the Hagen–Poiseuille equation defined as

$$\frac{\Delta p}{L} = \frac{\mu}{K}u + \frac{1}{2}C\rho u^2 \quad in[Pa/m] \qquad (7)$$

Where μ is the dynamic viscosity which is a function of the temperature, u is the velocity through the effective area of the porous medium in the x-direction, ρ is the density of the fluid, c is the inertial resistance, 1/K is the viscous resistance and d_h is the hydraulic diameter of each single passage that form the monolith. The pressure drop term is treated as an additional source term in the solution procedure of the discretized equations. The flow upstream and downstream the monolith is treated as turbulent and the low Reynolds version of the k–ε model are used for the turbulence modeling.

5.1.1 Problem Description

The nitrogen flows in through the inlet with a uniform velocity of 22.6 m/s, passes through a ceramic monolith substrate with square shaped channels, and then exits through the outlet. The solution is calculated for gas flow through the catalytic converter using the pressure based solver. The governing equations namely conservation of mass, momentum will be solved for analysis.. Intensity and hydraulic diameter specification method used for the turbulence model.

5.2 MESH FOR THE CATALYTIC CONVERTER GEOMETRY

A structured grid having 34930 computational nodes is used for the simulation of the computational domain. The geometry of the monolith is simulated with an individual cylinder block (shown between the diffuser and the nozzle of the computational configuration), which imposes to the fluid flow in the prescribed pressure drop.(See Figure 5.2) show the meshed geometry of the catalytic converter.

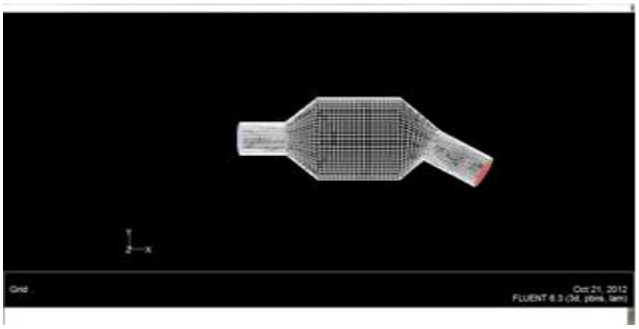

Figure 5.2 Mesh Geometry of Catalytic Converter

Grid sensitivity tests were conducted to illustrate the calculated pressure drop of the catalytic converter along x-direction at different velocities and mesh densities. The small deviations in the pressure drop values of increasing the mesh element densities indicated the reliability of the meshing scheme for further use.

5.3 VELOCITY VECTORS ON THE Y=0 PLANE

In the Figure 5.3 flow pattern shows that the flow enters the

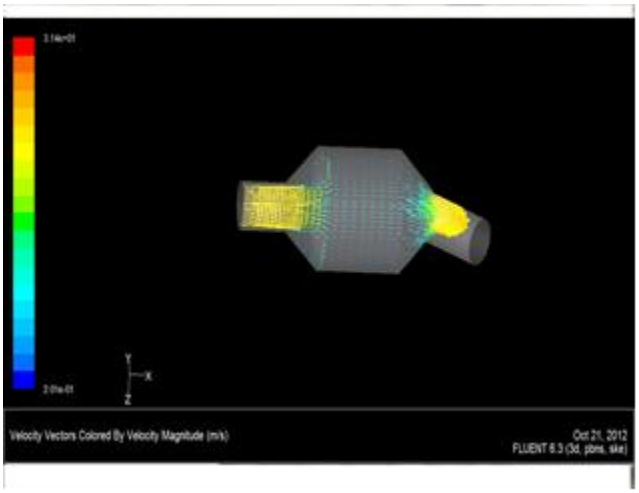

Figure 5.3 Velocity Vectors

catalytic converter as a jet, with recirculation on both sides of the jet. When it passes through the porous media,,it decelerates and straightens out, and performs a more uniform velocity distribution. This causes the metal catalyst present in the substrate to be more effective.

5.4 CONTOURS OF THE X VELOCITY ON THE X=95,X=130 & X=165 SURFACES

The (See Figure 5.4) shows the velocity profile becomes more uniform as the fluid passes through the porous media. The velocity is very high at the middle (the area in red) just before the nitrogen enters the substrate and then decreases as it passes through and exits the substrate. The por tion in green, which represents to a moderate velocity

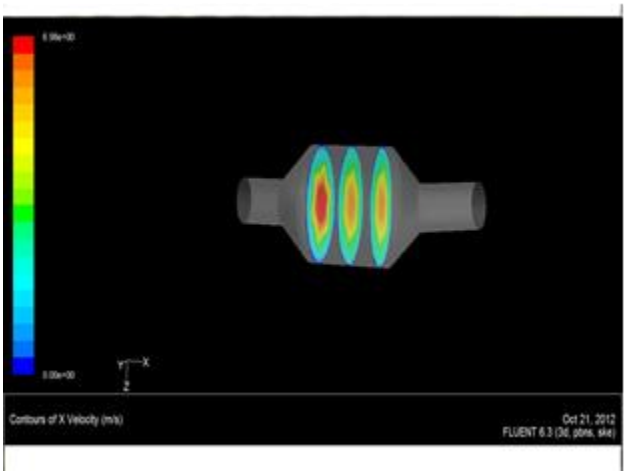

Figure 5.4 Contours Of X-Velocity

5.5 CONTOURS OF THE STATIC PRESSURE ON THE Y=0 PLANE

The (See Figure 5.5) shows that pressure changes rapidly in the middle section, where the fluid velocity changes as it passes through the porous substrate. The pressure drop can be high, due to the inertial and viscous resistance of the porous media. Determining this pressure drop is a goal of CFD analysis

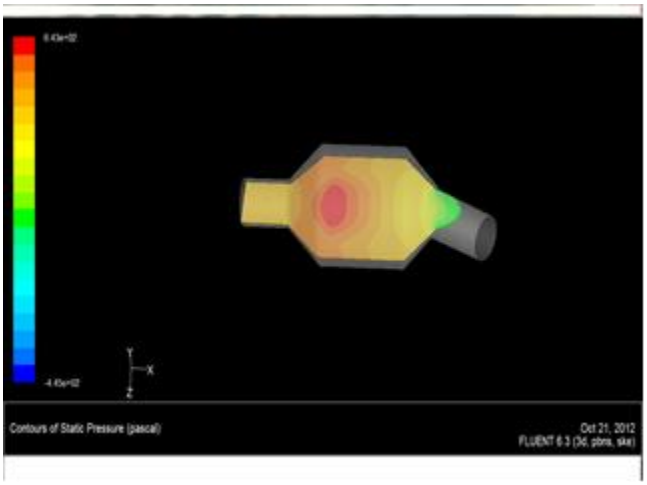

Figure 5.5 Contours Of Static Pressure

5.6 EFFECT OF VARIATION OF VISCOUS AND INERTIAL RESISTANCE ON PRESSURE DROP ACROSS THE SUBSTRATE

5.6.1 Case-I

(See Table 5.1) shows the inertial and viscous resistance at different directions for the substrate

Table 5.1Values For The Viscous And Inertial Resistance For Case-I

Direction	Viscous Resistance($1/m^2$)	Inertial Resistance($1/m$)
Direction-1	3.846e+07	20.414
Direction-2	3.846e+10	20414
Direction-3	3.846e+10	20414

In (See Figure 5.6), the pressure drop across the porous substrate can be seen to be roughly 300 Pa.

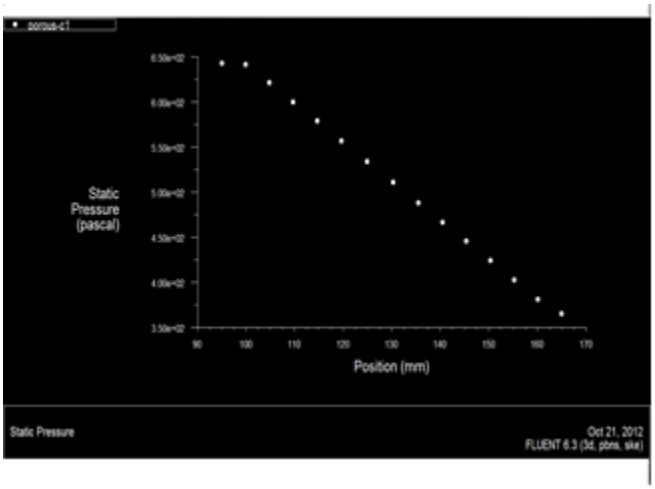

Figure 5.6 Static Pressure For Case-I

5.6.2 Case-II

(See Table 5.2) shows the inertial and viscous resistance at different directions for the substrate.

Table 5.2 Values For The Viscous And Inertial Resistance For Case-II

Direction	Viscous Resistance($1/m^2$)	Inertial Resistance(1/m)
Direction-1	3.846e+06	19.414
Direction-2	3.846e+09	19414
Direction-3	3.846e+09	19414

In (See Figure 5.7), the pressure drop across the porous substrate can be seen to be roughly 120 Pa.

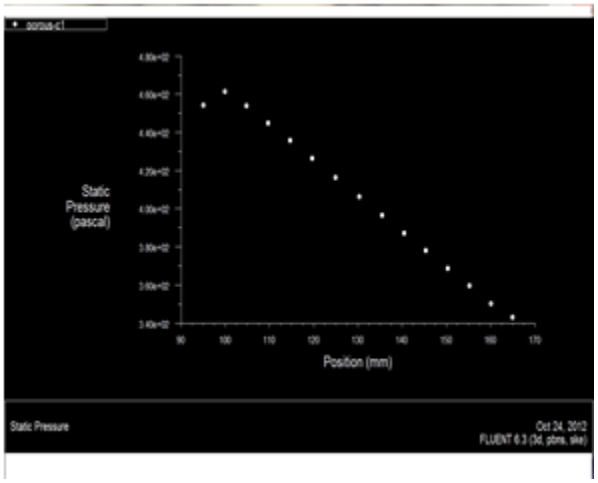

Figure 5.7 Static Pressure For Case-II

5.6.3 case-II

(See Table 5.3) shows the inertial and viscous resistance at different directions for the substrate

Table 5.3 Values For The Viscous And Inertial Resistance For Case-III

Direction	Viscous Resistance($1/m^2$)	Inertial Resistance(1/m)
Direction-1	3.846e+08	21.414
Direction-2	3.846e+11	21414
Direction-3	3.846e+11	21414

In (See Figure 5.8), the pressure drop across the porous substrate can be seen to be very high.

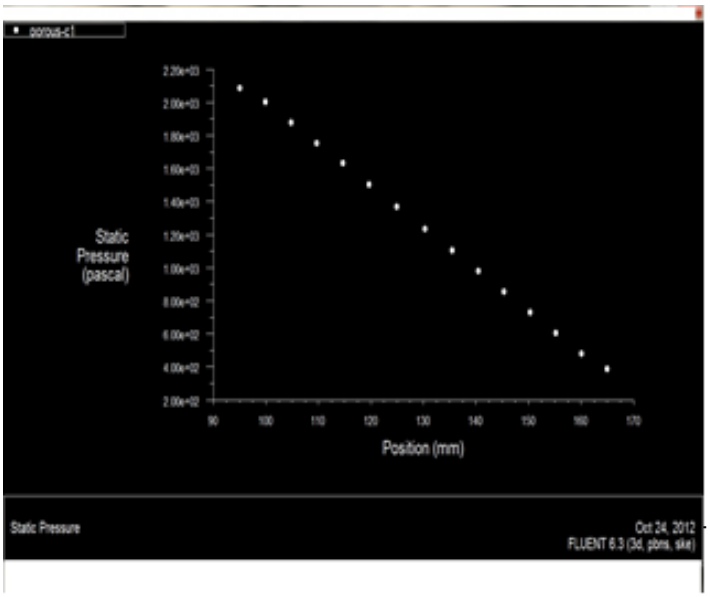

Figure 5.8 Static Pressure For Case-III

5.7 EFFECT OF MASS FLOW RATE (M) ON PRESSURE DROP ACROSS THE SUBSTRATE

The flow distribution is found to be more uniform inside a monolith brick with a lower inlet flow Reynolds number, a shorter inlet pipe, and a straight inlet pipe instead of a bent one. The flow through the monolith is treated as laminar and the pressure drop per unit length is calculated by Hagen–Poiseuille equation. From the (See figure5.10) it can be identify that pressure drop through a channel is an increasing function of the mass flow rate.

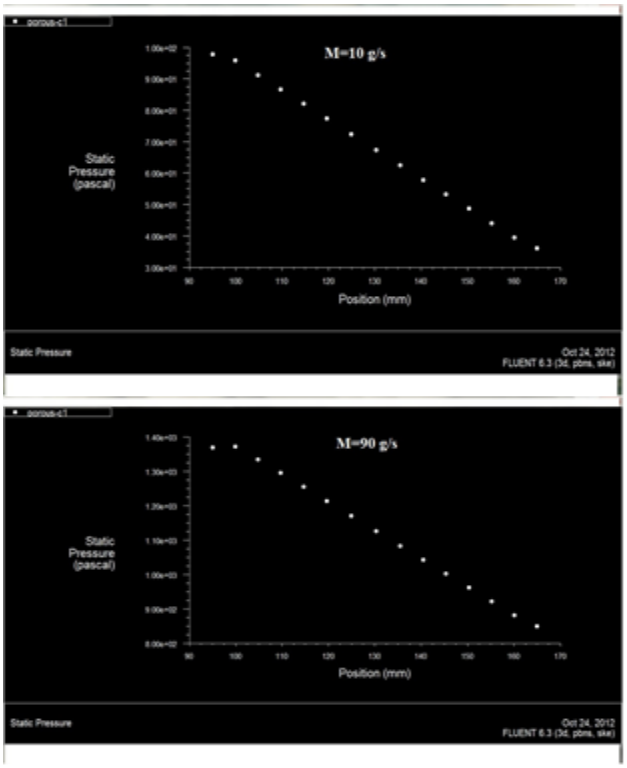

Figure 5.10 Pressure Drop With Mass Flow Rates

5.8 EFFECT OF INLET PIPE ANGLES

The maximum utilization of the catalyst volume would be achieved by having a uniform flow distribution through the monolith substrate. The velocity distribution on the inlet of substrate is shown in (See figure 5.11(a)-(d)). The velocity distribution for 30degree inlet pipe is highly non uniform on the substrate inlet. The velocity distribution for 45 degree inlet pipe is uniform on the substrate inlet. Since the cone angle is also 45 degrees, it guides the fluid to the substrate. The velocity distribution for 60 degree inlet pipe is also uniform, but peak pressure is high. Also, in this case an extra back pressure is observed as the higher angle acts as a flow restriction. The flow in the catalytic converter with appears to be less uniform for lower angles. The flow tends to create some additional backpressure for higher angles.[17]

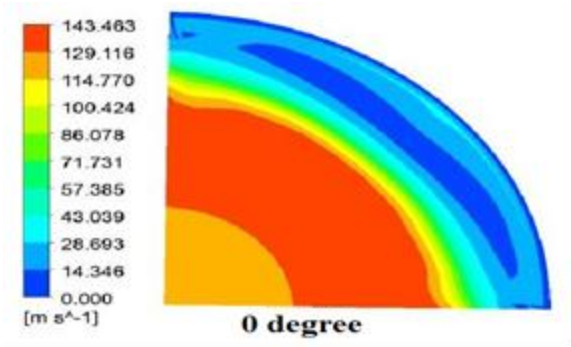

Figure 5.11(a)

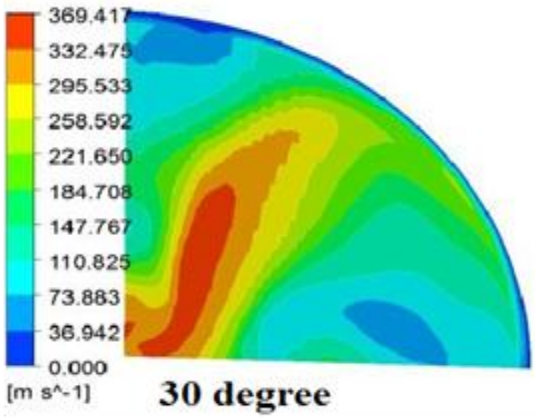

Figure 5.11(b)

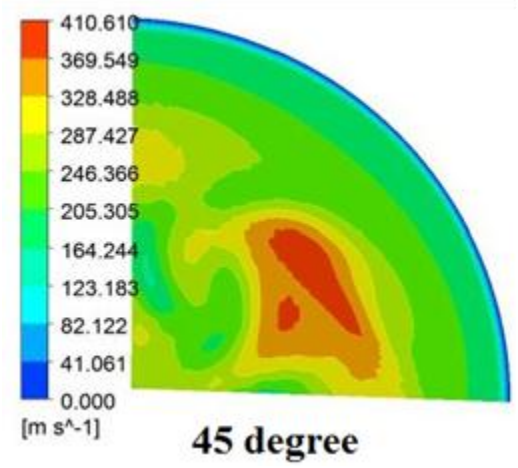

Figure 5.11(C)

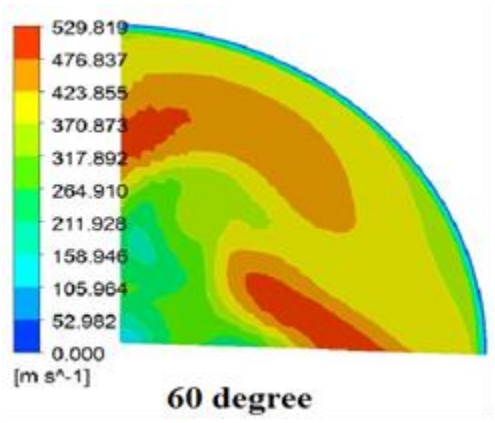

Figure 5.11(D)

6.CONCLUSION

The discussion on lowering the CO_2 emissions is omnipresent. Various solid materials like calcium oxide, hydrotalcite, zeolite etc. are readily adsorb carbon dioxide. The present work is to reduce CO_2 emissions by following methods (1) Enhancing the catalyst system to the engine performance and the back pressure (CFD Analysis) (2) Attaching chemical reagent coated adsorber system to the catalytic converter and thereby reducing CO_2 emissions from the exhaust. . A adsorber system of required size or configuration based on CFD results will be fabricated and tested with the either of above adsorbents.

REFERENCES

[1] HE LING, YU XIU-MIN, LI GUO-LIANG, XU NAN, "DYNAMIC RESPONSE OF A THREE-WAY CATALYTIC CONVERTER", ENERGY PROCEDIA 17 (2012) 547 – 554

[2] Halabi. M.H. , M.H.J.M. de Croon, J. van der Schaaf, P.D. Cobden, J.C. Schouten" High capacity potassium-promoted hydrotalcite for CO2 capture in H2 production", international journal of hydrogen energy 37 (2012) 4516-4525

[3] Michael Zammit and Jeffrey Wuttke,"The effects of Catalytic Location on Palladium Loading on Tailpipe Emissions", SAE international,2012-01-1247.

[4] Hayes. R.E, A. Fadic, J. Mmbaga, A. Najafi " CFD modelling of the automotive catalytic converter", Catalysis Today 188 (2012) 94–105

[5] Heechol Choi,Young Choon Park,Yong-Hyun Kim,and Yoon Sup Lee, "Ambient Carbon Dioxide Capture by Boron-Rich Boron Nitride Nanotube", J. Am. Chem. Soc. 2011, 133, 2084–2087.

[6] Joachim Braun, Thomas Hauber, Heike Többen and Peter Zacke "Influence of Physical and Chemical Parameters on the Conversion Rate of a Catalytic Converter: A Numerical Simulation Study", SAE International 2000-01-0211

[7] Wilfried Mueller, Joerg-Michael Richter, Marcus Schmidt and Martin Roesch, "Catalyst Technologies for Gasoline Engine with Respect to CO2 reduction", SAE international,2011 SIAT.

[8] Zhijuan Zhang, Wei Zhang, Xiao Chen, Qibin Xia, & Zhong Li, "Adsorption of CO2 on Zeolite 13X and Activated Carbon with Higher Surface Area", Separation Science and Technology, 45:5 (2010), 710-719

[9] Ankan kumar,Sandip Mazdar,"Toward simulation of full scale monolithic catalytic converters with complex hetrogeneous chemistry",Computers and Chemical Engineering 34 (2010) 135–145 .

[10] Akira Saito, Shigeru Ueki, Yayoi Nagatomi, Naoya Sawazu and Yutaka Takada, "Analysis of CO2 Reduction Mechanism with light Duty Diesel Freight Vehicle in Real traffic Condition", SAE international,2008-01-1304.

[11] Valentinas Mickunaitis, Alvydas Pikunas & Igor Mackoit (2007):"Reducing fuel consumption and CO2emission in motor cars", Transport, 22:3, 160-163.

[12] US Patent 2007 Conversion of carbon monoxide using cobalt-based metal oxide catalysts, source:www.patentstorm.us/patents/5502019.html (7/5/2007)

[13] Moreira R. F. P. M. , J. L. Soares, G. L. Casarin & A. E. Rodrigues (2006): "Adsorption of CO2 on Hydrotalcite-like Compounds in a Fixed Bed", Separation Science and Technology, 41:2, 341-357.

[14] Silva.C.M.,Costa.M,T.L.Faris,H.santos,"Evaluation of SI engine exhaust gas emissions upstream and downstream of the catalytic converters", Energy Conversion and Management 47 (2006) 2811–2828.

[15] Abhijit R Dake, "Modeling and control of cold start hydrocarbon emissions", Phd dissertation, 2005

[16] Yuji Tsushima, Shunji Akamatsu and Yoshihiro Takada, "Fuel Economy Improvement and CO2 Reduction of Motorcycle Gasoline SI Engine and Its Simulation", SAE Paper, 990017, 1999.

[17] Wendland, D. W., Sorrell, P. L. ,and Kreucher, J. E.,"Sources of Monolith Catalytic Converter Pressure Losses", SAE Paper 912372, 1991.